NUMERICAL SIMULATION OF THE FLUORESCENCE INDUCTION IN PLANTS

BY

Alexandrina D. STIRBET* & Reto J. STRASSER**

ABSTRACT

Numerical simulation of the fluorescence induction in plants. - The variable fluorescence in the fast phase of chlorophyll a fluorescence induction phenomenon is closely related to the electron in photosystem II (PS II) of plants, algae and cyanobacteria. We present here two theoretical models that simulate successfully the experimental data on the O-J-I-P fluorescence transient using PS II reactions. The "core" of both these proposed theoretical models are charge stabilization and the two-electron-gate process on the acceptor side of PS II. The assumptions include: (1) PS IIs are homogeneous; (2) PS IIs are unconnected; and (3) the redox reactions of PS II obey a first order kinetics. The two models tested are: (1) individual (in which the electron carriers Q_A and Q_B have been considered to function as individual entities); and (2) complex (in which the electron carriers Q_A and Q_B have been considered to function in pairs in the PS II reaction center complexes).

Data for dynamic analysis of both models were obtained through numerical integration of the Ordinary Differential Equations (ODE). Livermore Solver of Ordinary Differential Equations with Method Switching (LSODA) procedure was included in a specialized simulation software Gepasi. We have considered as input parameters the initial concentrations of reactants and the rate constants for redox reactions.

We have also verified our theoretical models by simulating fluorescence transients under three different experimental conditions: (1) variation of the light intensity; (2) DCMU treatment; and (3) re-exposure of the samples to actinic light after a defined period of darkness (double-hit experiments). The theoretical curves obtained converge quite well toward the experimental ones, proving that the redox reactions considered in our models are adequate for describing the fluorescence induction phenomenon, and that the numerical simulation by using highly developed programs is a powerful tool to investigate the dynamics of the primary reactions of photosynthesis.

Key-words: Photosynthesis, chlorophyll a fluorescence, fluorescence induction, numerical simulation, mathematical modeling.

INTRODUCTION

The study of chlorophyll a fluorescence (a non invasive and intrinsic probe for the photosynthetic apparatus) has generated a large amount of data regarding mechanisms involved in photosynthesis, /1-4/. A special effect, that is still incompletely understood, even though it was observed as early as 1931, /5/, is represented by the Kautsky effect,

*University of Bucharest, Faculty of Physics, Department of Biophysics, P.O. Box 5211, R-76900, Bucharest, Romania.
**University of Geneva, Bioenergetics Laboratory, CH-1254 Jussy, Geneva.

TABLE 1

The redox reactions taken into consideration in the two proposed theoretical models: complex model and individual model.

COMPLEX MODEL [QaQb]		INDIVIDUAL MODEL [Qa] + [Qb]	
R 1	$QaQb \rightarrow Qa^-Qb$		
R 2	$QaQb^- \rightarrow Qa^-Qb^-$		
R 3	$QaQb^{2-} \rightarrow Qa^-Qb^{2-}$	$Qa \rightarrow Qa^-$	R I
R 4	$QaQbH_2 \rightarrow Qa^-QbH_2$		
R 5	$QaU \rightarrow Qa^-U$		
R 6	$Qa^-Qb \rightleftharpoons QaQb^-$	$Qa^- + Qb \rightleftharpoons Qa + Qb^-$	R II
R 7	$Qa^-Qb^- \rightleftharpoons QaQb^{2-}$	$Qa^- + Qb^- \rightleftharpoons Qa + Qb^{2-}$	R III
R 8	$QaQb^{2-} \rightleftharpoons QaQbH_2$		
R 9	$Qa^-Qb^{2-} \rightleftharpoons Qa^-QbH_2$	$Qb^{2-} \rightleftharpoons QbH_2$	R IV
R 10	$QaQb^- \rightarrow QaQb$		
R 11	$Qa^-Qb^- \rightarrow Qa^-Qb$	$Qb^- \rightarrow Qb$	R V
R 12	$QaQbH_2 \rightleftharpoons QaU + PQH_2$		
R 13	$Qa^-QbH_2 \rightleftharpoons Qa^-U + PQH_2$		
R 14	$QaU + PQ \rightleftharpoons QaQb$	$QbH_2 + PQ \rightleftharpoons Qb + PQH_2$	R VI
R 15	$Qa^-U + PQ \rightleftharpoons Qa^-Qb$		
R 16	$PQH_2 \rightleftharpoons PQ$	$PQH_2 \rightleftharpoons PQ$	R VII

also known as fluorescence induction or fluorescence transient. This effect is characterized by a specific variation in time of the fluorescence intensity upon light exposure of the photosynthetic apparatus following a period of darkness. This transient is over in no more than several minutes, after which the fluorescence intensity is found to reach a steady state value.

In the first moments, upon the light exposure, fluorescence rises from an initial minimal value, F_0, to a maximal value, F_p, with two intermediate steps J and I, /6-8/. This is followed by the so called slow phase, when the fluorescence intensity diminishes to a low value T (or F_s) which is close to the value at F_0. Since the chlorophyll concentration remains unchanged during the time of these measurements, the variation in time of the fluorescence intensity has been considered to be due to the variation of the quantum yield of fluorescence emission (between 2% and 10%), /9, 4/.

TABLE 2

The values of the rate constants of redox reactions utilized in numerical simulation with individual model and complex model. k1 and k2 are the rate constants for forward and reverse reactions respectively.

COMPLEX MODEL [QaQb]			INDIVIDUAL MODEL [Qa] + [Qb]		
	k1[s⁻¹]	k2[s⁻¹]		k1[s⁻¹]	k2[s⁻¹]
R 1	1500	-			
R 2	1500	-			
R 3	1500	-	R I	1500	-
R 4	1500	-			
R 5	1500	-			
R 6	1500	150	R II	1500	150
R 7	2000	40	R III	2000	40
R 8	100	100	R IV	100	100
R 9	100	100			
R 10	4000	-	R V	4000	-
R 11	4000	-			
R 12	100	100			
R 13	100	100	R VI	100	100
R 14	100	100			
R 15	100	100			
R 16	1	-	R VII	1	-

The interpretation of this fluorescent transient has been the subject of a large number of published papers, /1, 2, 8/, based either on experimental data or theoretical analysis. We now know a great deal about the primary processes of the photosystem II, that are linked to fluorescence transient: excitation energy transfer, and charge separation, /4, 10-12/. A good approach and the understanding of the relationship between fluorescence transient to the primary events in photosystem II (PS II), seems to be the mathematical modeling of the assumed biochemical reactions involved, and the comparison of the theoretically obtained results with the experimental data, as has been attempted by Strasser, /11/, or by Trissl and coworkers, /12/. In this respect, the fast phase of the fluorescence transient, in the millisecond time scale, has been linked to several redox reactions. Previous models have focused either on the charge stabilization reaction (DCMU experiments), /12, 13/, or on the two-electron gate process, /14-17/. In the present work we use a mathematical model of PS II that simulates the O-J-I-P

TABLE 3

The values of various parameters (rate constants — k1 and k2, equilibrium constant — K_{eq}, and half-time-$t_{1/2}$) of redox reactions of PS II.

Reactions	k or $t_{1/2}$	K_{eq}	References
$QaQb \rightarrow Qa^-Qb$	$k = 23.3 s^{-1}$ (at 1 W/m²)		15
	$k = 150 s^{-1}$ (at 40 W/m²)		14,17
	$k = 105 s^{-1}$ (at 28 W/m²)		14,17
	$k = 75 s^{-1}$ (at 20 W/m²)		14,17
$Qa^-Qb \rightarrow QaQb^-$	$t_{1/2} = 100\text{-}200\,\mu s$	3.5 (basic) 98 (acid)	34
	$t_{1/2} = 200\text{-}400\,\mu s$		35
		15-20	36
	$k_1 = 4600 s^{-1}; k_2 = 460 s^{-1}$	10	15
	$k_1 = 3500 s^{-1}; k_2 = 175 s^{-1}$	20	14,17
$Qa^-Qb^- \rightarrow QaQb^{2-}$	$t_{1/2} = 400\text{-}600\,\mu s$	50	36
	$t_{1/2} = 600\text{-}800\,\mu s$		35
	$k_1 = 1400 s^{-1}; k_2 = 28 s^{-1}$	50	15
	$k_1 = 1750 s^{-1}; k_2 = 35 s^{-1}$	50	14,17
	$k_1 = 1750 s^{-1}; k_2 = 1750 s^{-1}$	1	14,17,37
$QbH_2 + PQ_{pool}$ $\downarrow$ $Qb + PQH_{2pool}$	$t_{1/2} = 1ms$		15,33,38,39
		1	14,36,37
	$k_1 = 100 s^{-1}; k_2 = 100 s^{-1}$	1	15
	$k_1 = 30 s^{-1}; k_2 = 30 s^{-1}$	1	17
PQH_{2pool} $\downarrow$ PQ_{pool}	$t_{1/2} = 12\ ms; t_{1/2} = 100\ ms$		33
	$k = 1$		17

curves of variable fluorescence (as measured in /6-8/). Moreover, this theoretical model has been tested by simulation of the fluorescence induction obtained under different experimental conditions: variation of light intensity, DCMU treatment at different light intensities, and re-exposure of the samples to actinic illumination after a defined dark period (double-hit experiments).
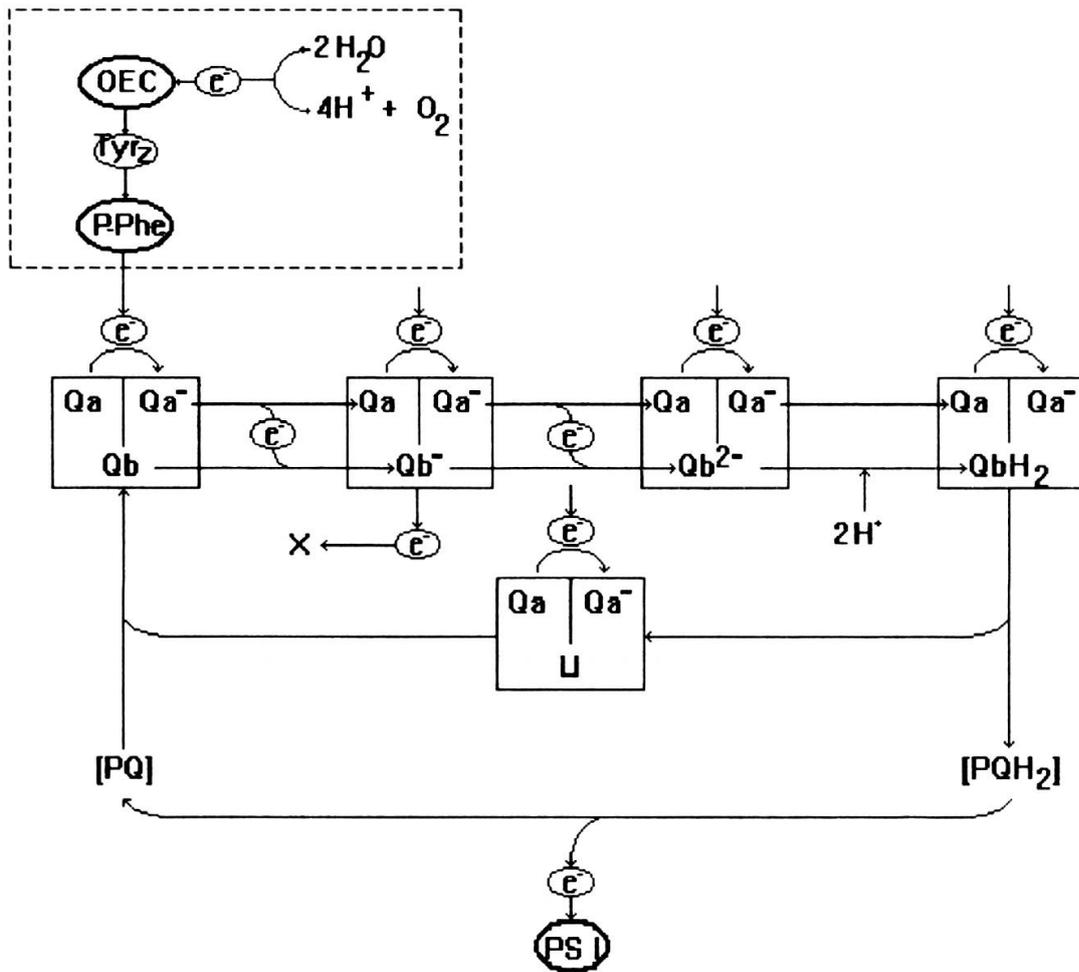
FIG. 1.

Scheme of the electron transport reactions considered in the theoretical models. OEC: oxygen evolving complex. Tyr_Z: primary electron donor to $P680^+$. P: reaction center P680. Phe: pheophytin a. Q_A: primary bound plastoquinone. Q_B: secondary bound plastoquinone. X: unknown electron acceptor. PQ:

THEORETICAL APPROACH

As the variable fluorescence is mostly due to the variations of fluorescence emission associated with the antenna chlorophyll of photosystem II (see reviews in Govindjee et al., /18/), we have considered only this photosystem in our theoretical approach. In the first approximation we assume a homogeneous population of PS II, without excitation transfer between different photosystems (separate unit model), /19/. It is well known that during exposure of a green plant to light, of an intensity higher than 100 W/m², the primary quinone acceptor (Q_A) accumulates in its reduced form (Q_A^-).
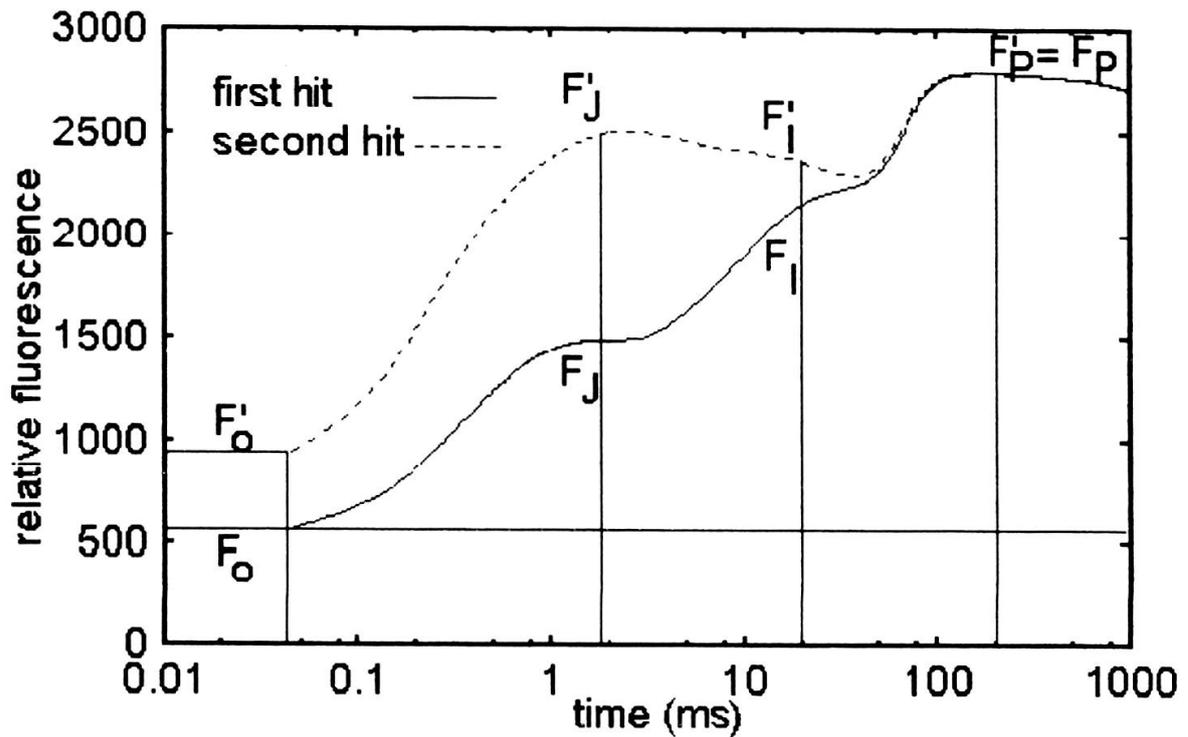
FIG. 2.

The fast phase of chlorophyll a fluorescence induction in plants: first illumination (first hit) of dark adapted plants, and second illumination (second hit) after 10 s of darkness. Experimental data obtained with a shutter-less system (Plant Efficiency Analyzer built by Hansatech Ltd.). (Also see /8/).

The net Q_A^- accumulates as the plastoquinone molecules of the PQ pool become reduced (the reoxidation of plastoquinone by Cyt b_6/f being the limiting reaction of the linear electron transport chain, /20, 21/). The area above the fluorescence curve relative to the maximal fluorescence reflects the number of electrons that are transported through PS II, /22/. Since oxidized Q_A is a strong quencher for the PS II fluorescence, /23/, the accumulation of the reduced Q_A seems to be the main factor that must be considered when the fluorescence induction is analyzed.

The reaction center Chl a of PS II in its oxidized state, P680+, is also an efficient fluorescence quencher, /24-26/, the excitation energy transferred by antenna pigments to this cation has been suggested to dissipate rapidly through internal conversion to heat. Under normal conditions there is no significant accumulation of P680+, as the abundant water molecules keep it reduced via the Mn complex and the intermediate Z (tyrosine), /4/. However, "in vitro", under continuous illumination, accumulation of P680+ can occur, when the oxygen-evolving complex of PS II is inhibited by exogenous chemicals or heat treatment, /4, 27, 28/. In the present stage of our model we consider only indirectly the electron donor side of PS II.
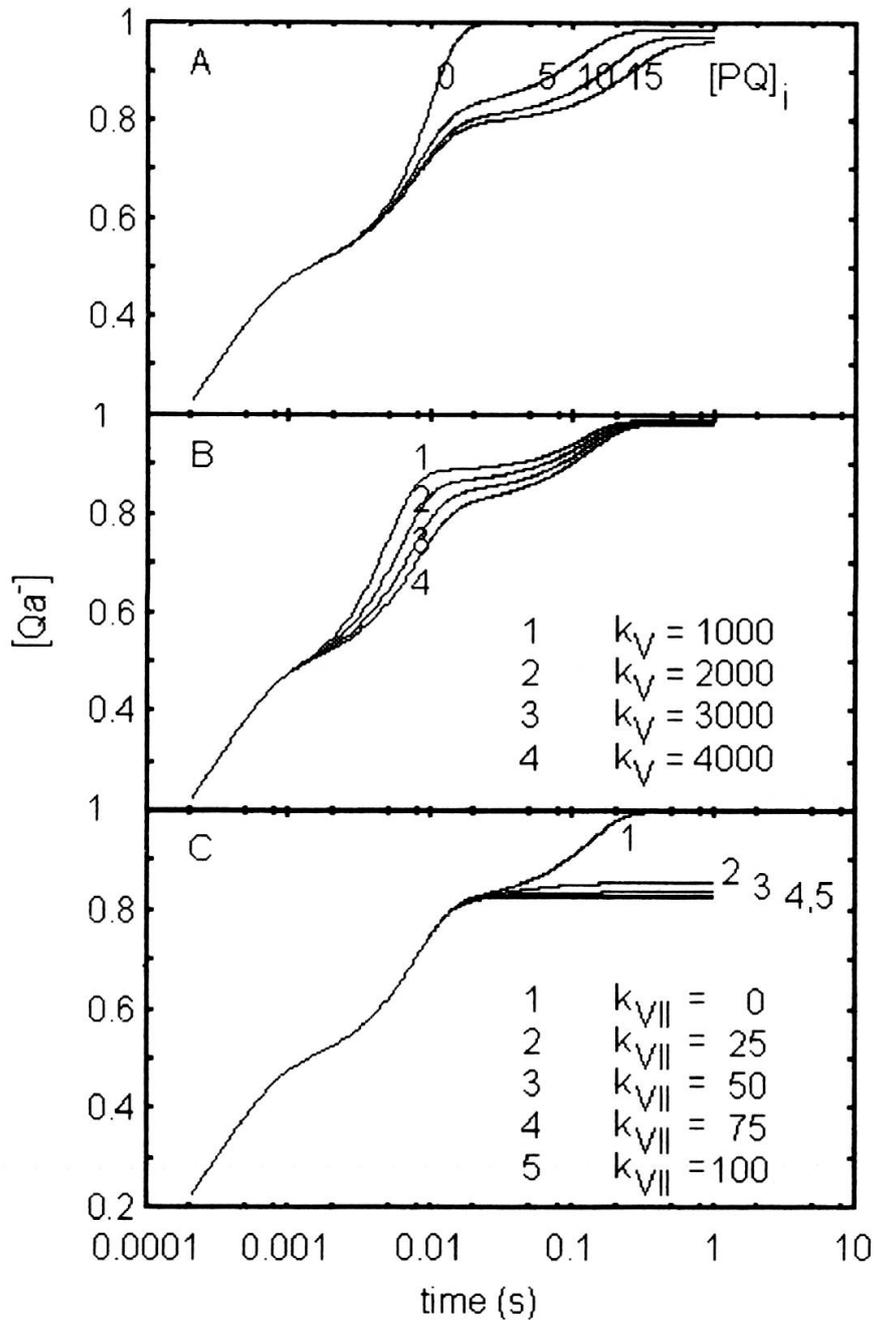
FIG. 3.

The numerical simulated curves obtained with the individual model by modifying different initial parameters (if not mentioned the parameters have the values indicated in Table 2). **A**: variation of the initial number of plastoquinone molecules in PQ pool. **B**: variation of the rate constant of reaction **V** (the electron transfer from Q_B^- to an unidentified compounds X). **C**: variation of the rate constant of reaction **VII** (reoxidation of PQH_2).

We assume here that the Q_A^- concentration is proportional to the variable fluorescence intensity. In Figure 1 a diagram of electron transfer reactions, involving the "two-electron gate", used in our numerical integration, is shown. The connection of the

Fig. 4.

The numerical simulated curves obtained A: with individual model, and B: with complex model. The utilized rate constants of the reactions are those presented in Table 2. Only curves 1 and 2 are directly comparable between Figures **A** and **B**.
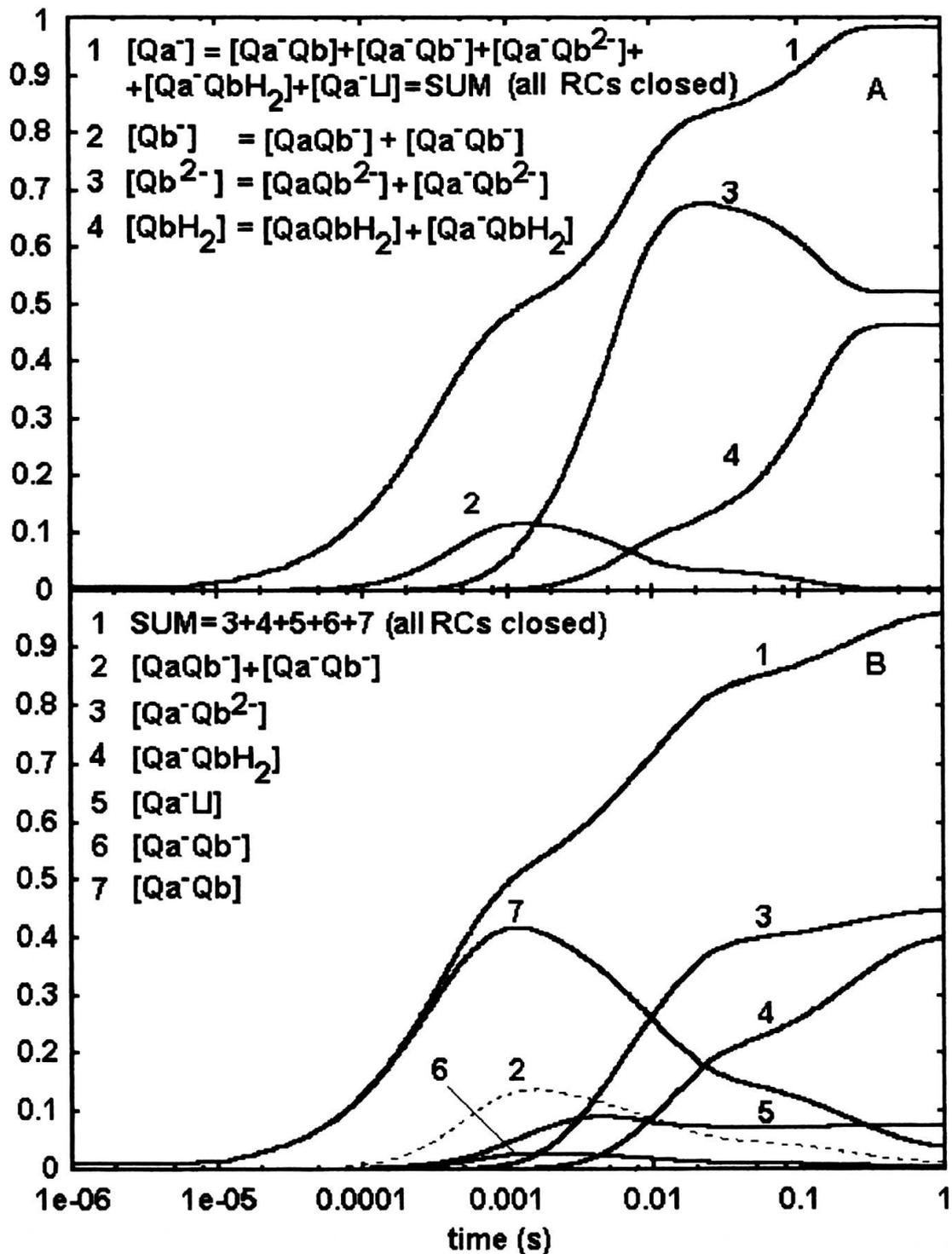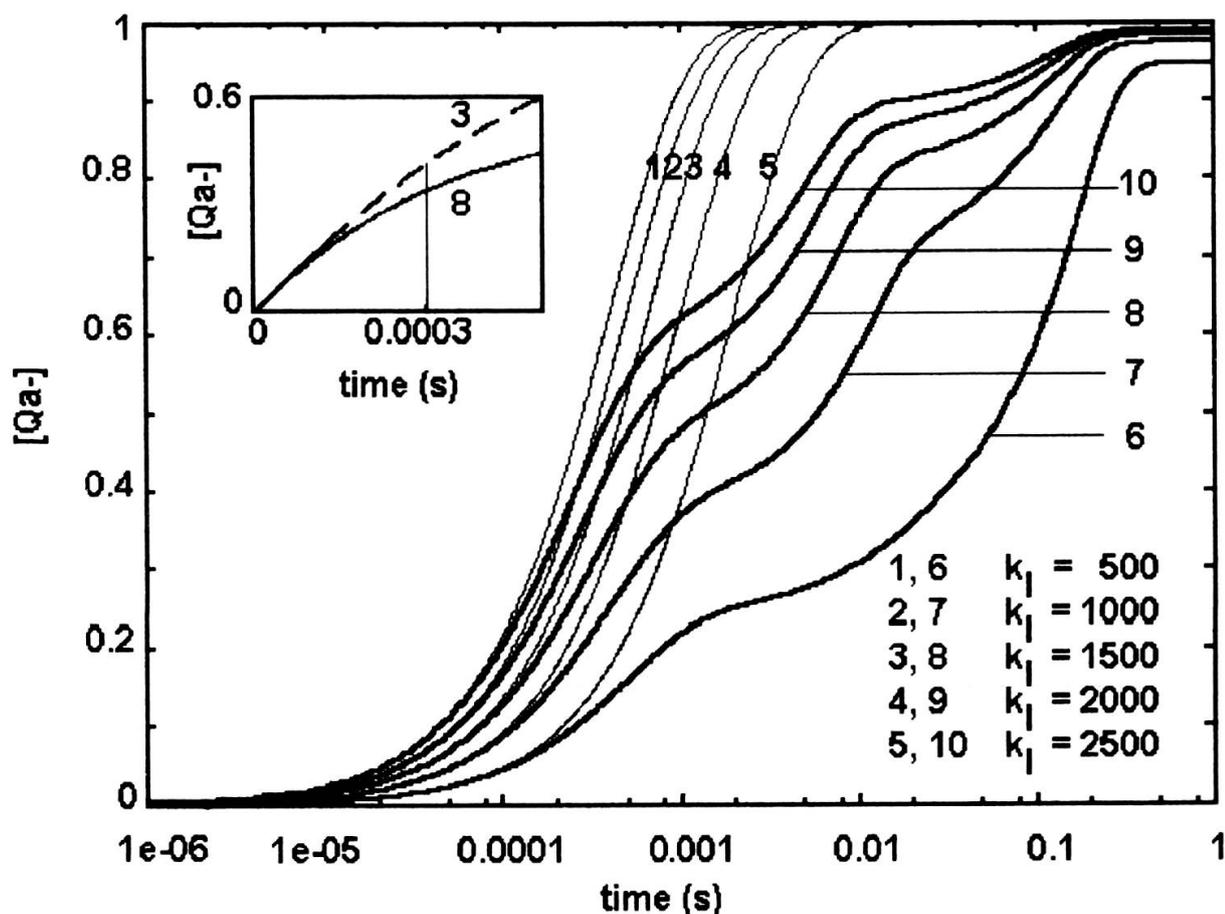
FIG. 5.

The numerical simulated curves obtained with the individual model for different light intensities (different rate constants of the reaction **I** — reduction of Q_A). 1-5 curves: fluorescence transients of DCMU treated plants; 6-10 curves: fluorescence transients of untreated plants. The insert shows that already at an early stage (e.g., 50 to 300 μs) the slope of the curve with DCMU is appreciably higher than without DCMU, even though the theoretical slope at the origin is the same for both curves.

reaction center P680 with the acceptor side of PS II is made through the reduction of Q_A via Pheophytin (Phe), while the oxidation of plastoquinol by Cyt b_6/f complex allows the connection of PS II with PS I.

Our computation has been made in two ways: (1) using the so called "individual model", where electron carriers Q_A and Q_B have been considered as individual entities; and (2) using a "complex model", where we take into consideration the fact that Q_A and Q_B are to be found stoichiometricaly 1:1 (pairs) in most PS II reaction center complexes. In Table I the redox reactions for these two models are presented (reactions **1-16** for the complex model, and **I-VII** for the individual model). Reactions **1-5** (Q_A reduction) are similar with the reaction **I**, and reactions **12-15** (removal of PQH_2 from the complex, and binding of PQ at the complex) are represented by the global reaction
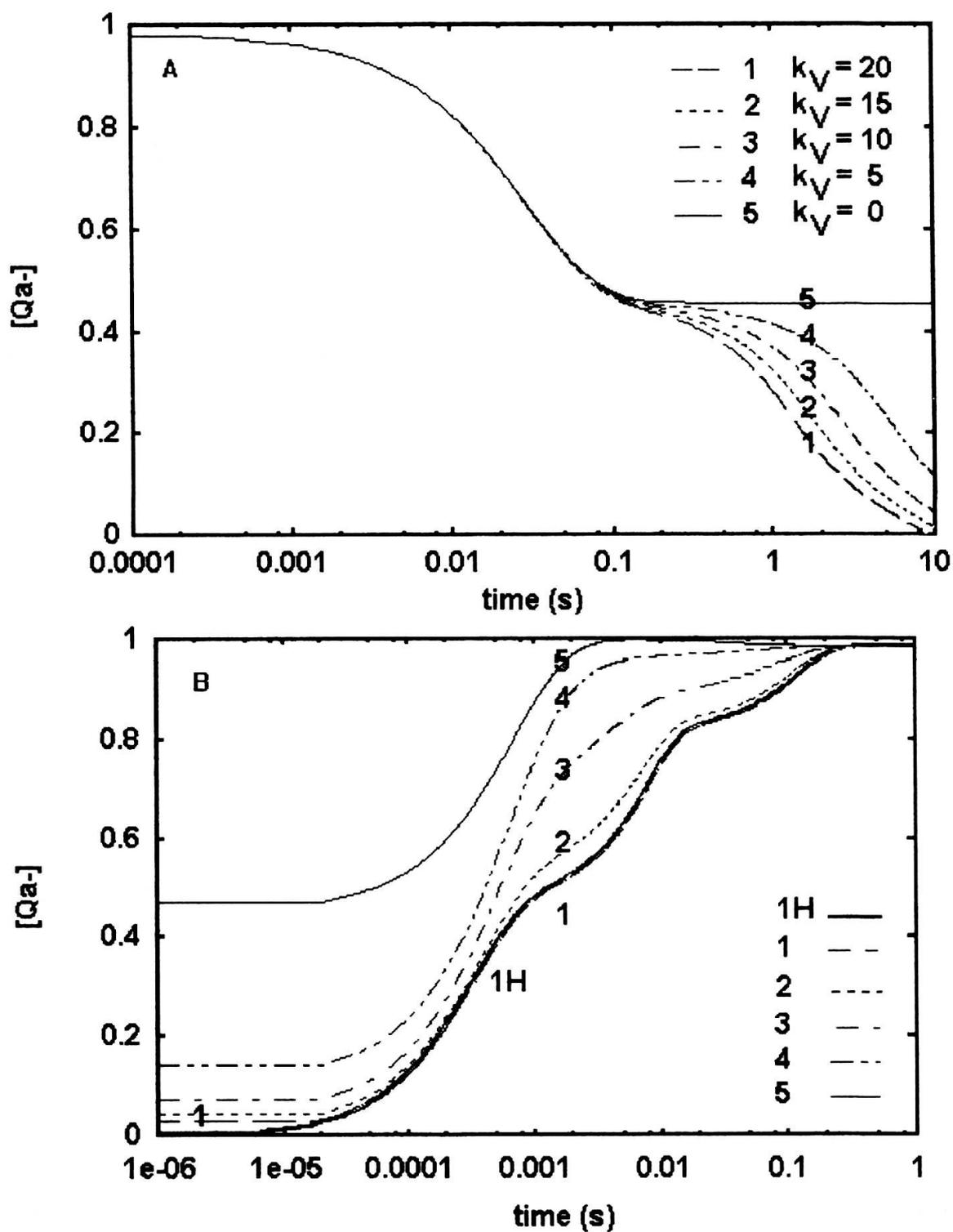
FIG. 6.

The numerical simulation with the individual model of a double hit experiment for different values of the rate constant of reaction **V** (the electron transfer from QB– to an unidentified compound X) in the dark period. **A**: 1-4 curves — the fluorescence decays in darkness after 1 sec of illumination; **B**: 1H curve — the first fluorescence transient. 1-4 curves — the second fluorescence transients after 10 sec of darkness.
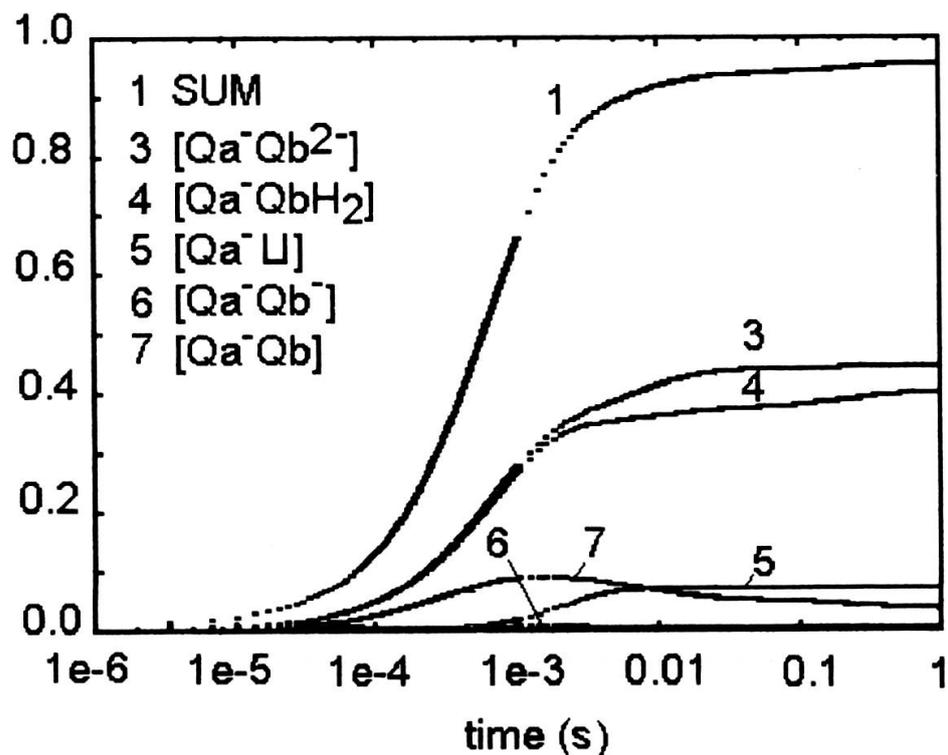
FIG. 7.

The numerical simulated curves obtained with the complex model for the second illumination after 10 sec of darkness. The rate constant of the reaction **9** (the electron transfer from Q_B^- to an unidentified compound X) in darkness was 5 s^{-1}.

VI in the individual model. The theoretical value of the variable fluorescence intensity, at any time, is considered to be the value of the Q_A^- concentration. For the complex model that means the sum of the all five redox forms of the reaction center complex ($Q_A^-Q_B$, $Q_A^-Q_B^-$, $Q_A^-Q_B^{2-}$, $Q_A^-Q_BH_2$, and Q_A^-U). In this respect, the results have been more easily obtained with the individual model, in which the concentration of Q_A^- is directly calculated.

Our results do not show strong qualitative differences for the two models, primarily because the major determinant for fluorescence yield changes in both cases is Q_A^- concentration. Thus, the individual model is also adequate, in spite of its simplicity.

NUMERICAL SIMULATION

Gepasi version 2 software, /29/, connected to a graphical package (GNUPLOT version 3.5, /30/) and running under MS-Windows on an IBM PC, has been used to generate all curbes corresponding to our theoretical models. With this software, the data

for the dynamic analysis of the models are obtained through numerical integration of the ordinary differential equations system (ODE) — derived in a classical treatment applied to the redox reactions considered — describing time changes of the reactant concentrations. In a first approximation, we have considered that the chemical kinetics for the reactions is of mass action type. The numerical algorithm used is the Livermore Solver of Ordinary Differential Equations with Method Switching (LSODA) procedure, /31/, which detects if the ODE system is stiff or not /32/ and then makes use of the most efficient method for numerical integration — Adams or BDF (Backward Differentiating Formula) /33/.

RESULTS AND DISCUSSIONS

During exposure to saturating light at room temperature, chlorophyll a fluorescence of dark-adapted green plants show, in a semilogarithmic representation (log time), a multiphasic variation characterized by the O-J-I-P sequence (see Figure 2 showing two curves), where F_0 is the initial value of the emitted fluorescence, F_P is the maximum fluorescence obtained, while F_J and F_I are two intermediate stages.

The numerical simulation with Gepasi software of these experimental curves requires the utilization, as input parameters, of the initial concentrations of the reactants, as well as of the rate constants for the redox reactions corresponding to the two models — individual and complex. To understand the way these parameters could affect the shape of the generated curves, characteristic results, obtained in the numerical simulation of the individual model are shown in Figure 3. Except for the values mentioned in the figure, the values of the initial parameters have the values indicated in Table 2.

In Figure 3A the time dependence of Q_A^- curves, obtained for different sizes of the PQ pool (respectively 0, 5, 10 and 15 molecules) are shown. It can be seen that the time interval between I and P increases with the number of PQ molecules, while the maximum fluorescence P decreases. Thus, by changing this parameter we can modify drastically the form of the O-J-I-P curves. In a linear time representation of the results it can be easily seen that the area over the fluorescence curve is proportional to the size of the PQ pool, in agreement with predictions from the literature, /22/. We realize that for the fitting of our theoretical models with the experimental data, the knowledge of the exact number of PQ molecules in our sample is very important, as was already shown by Hsu, /15/.

Another example is given in Figure 3B, where the results obtained with different values of the rate constant for the reaction **V** are shown. The reaction **V** is a characteristic electron transfer from Q_B^- towards an unidentified compound (X in our models).

We have introduced this reaction to modify the initiation time of the step I, which is shifted from 8 ms to 30 ms, as this rate constant change from 0 to 4000. Moreover, experiments with modulated fluorescence techniques bring evidences about the supposed existence of such an electron acceptor X (unpublished results).

An interesting result has been obtained by changing the value of the rate constant corresponding to reaction **VII** (reoxidation of PQH_2). In Figure 3C we show that following an initial modification from 0 to 25 in the rate constant of this reaction there is no further differentiation between the steps I and P. These types of curves have been obtained experimentally with light-adapted plants (see Fig. 4B in /8/), in which the State 1-State 2 transition was achieved. We can suppose that after this transition, that leads to changes in thylakoid structure and ion redistribution, the connection between the two photosystems is improved. The studies of Joliot and Joliot, /34/, prove that the rate of electron transfer from PS II to PS I is limited neither by the diffusion nor by the binding of plastoquinol to Cyt b_6/f complexes, but by electron transfer processes occurring within the Cyt b_6/f complexes, and that the rate of these limiting processes is very likely controlled by the redox state of the high potential chain (cytochrome f and Rieske protein).

In Figure 4A we present the numerical simulation with the individual model. Curve 1 (the O-J-I-P theoretical curve) gives the time dependent variation in of Q_A^- concentration (all RCs closed), and the curves 2-4 give the time dependent variation in concentrations of the Q_B^-, Q_B^{2-} and Q_BH_2, respectively. We have found a specific distribution in time of the reduced Q_B forms: Q_B^- appears to be predominant at the J step. However, only very little of the Q_B^- belongs to the closed complex $Q_A^-Q_B^-$ (see curves 2 and 4 in Figure 4B, which is from the complex model). Therefore, the fluorescence intensity observed at the step J is mainly due to the presence of $Q_A^-Q_B$ (compare curve 7 with curves 2, 5 and 6 in Figure 4B). Q_B^{2-} dominates at the I step, while a mixture of Q_B^{2-} and Q_BH_2 is built up at the P step. The input parameters have been so adjusted that the initiation times as well as the corresponding amplitudes for J, I and P steps have values comparable to the experimental ones.

The results shown in Figure 4B are obtained from the simulation by the complex model. Curves 3-7 show the changes in time of the concentrations of the reaction center complexes (RC) with Q_A in its reduced form: $Q_A^-Q_B$, $Q_A^-Q_B^-$, $Q_A^-Q_B^{2-}$, $Q_A^-Q_BH_2$, and Q_A^-U (complex without Q_B), respectively. Curve 1 simulates the variable fluorescence, obtained as the sum of concentrations of the five redox forms of closed RCs. We found that $Q_A^-Q_B$ is predominant at the J step. At the I and P steps all five RC forms are found in a mixture, $Q_A^-Q_B^{2-}$ and $Q_A^-Q_BH_2$ being predominant. The $Q_A^-Q_B^-$ concentration is quite small, due to the reactions **10** and **11** (oxidation of Q_B^- by X), and its maximum value is obtained in approximately one millisecond (the time domain of J step).

Thus, both the models, individual and complex, can simulate an O-J-I-P profile. Also, the distribution in time of the different redox forms of reactants is similar in the two models. The main contribution of $Q_A^-Q_B$ at the J step, the presence of Q_B^- (mainly in the open form as $Q_AQ_B^-$) only at the J step, and the mixture of the redox forms $Q_A^-Q_B^{2-}$ and $Q_A^-Q_BH_2$ at the I and P steps are obtained. The main differences in the kinetic results obtained with these models are related to the exchange process of Q_B with the PQ pool (reactions **12-15** in the complex model, and reaction **VI** in individual model). The time of reaching the P level is slower for the complex model, when the rate constants of the reactions **12-15** and **VI** have the values presented in Table 2.

The rate constant values utilized in numerical integration have been chosen as the J, I and P steps become visible, and have the initiation times and intensisies close to the experimental measured values. In this work we do not intend to evaluate the precise values of these constants by fitting theoretical curves with experimental ones. However, by comparing Table 2 (with the rate constant values of the redox reactions utilized in our simulations) and Table 3 (with the rate constant values of the redox reactions found in the literature), it can be seen that, generally, they are of the same order of magnitude.

The simulations of the O-J-I-P curve in itself do not prove the validity of our theoretical models. They could be validated partially if the rate constants used agree with the experimentally measured ones. A further verification would be achieved if our models could simulate the results obtained in experiments in which some external parameters are varied. We have therefore chosen to tests our model with other data on green plants, /8/: i) in the presence of DCMU (that substitutes Q_B and impairs reoxidation, /41/), ii) transient upon exposure to different light intensity and iii) transient after a second excitation (that we call double hit experiments).

Figure 5 shows the results obtained from the simulation by the individual model of the fluorescence induction curves of plants treated with DCMU (the value of the rate constant for reaction **II**, electron transport from Q_A^- to Q_B, is zero). Curves 1-5 correspond to different light intensities (the rate constant for reaction **I**, Q_A to Q_A^- reaction, has values from 500 to 2500). From our models the fluorescence has been found to have an exponential shape and the saturation time to be inversely proportional to the light intensity. We have attributed to the rate constant of the reaction **I** a value that leads to saturation in a time interval similar to the experimentally observed one (1-2 ms, for the light intensity of 600 W/m^2, /8/).

Figure 5, curves 6-10, also shows, simulated by the individual model, the O-J-I-P curves obtained as a function of the light intensity (rate constant for reaction I has values from 500 to 2500). It can be seen that the intermediate J, I and P steps are specifically dependent on the light intensity. The initiation times are shorter (with

higher amplitudes) at higher intensities. These results fit quite well with the experimental results for medium light intensity, /8/. However, at low light intensity (k = 500) J is still quite well apparent on the simulated curve, while I is almost superimposed by P in the ascending region of the curve. This is in disagreement with the experimental data in which I is easily identified, J being less visible (see Fig. 3B in /8/).

Our simulation of double hit experiments (for which the illumination is repeated after a relatively short period of darkness following the first light exposure) took into consideration two new steps: the fluorescence decay corresponding to the dark period and then the increase in fluorescence as a result of the second light exposure. In the dark step we considered a zero value for the rate constant corresponding to the reaction **I** (reduction of Q_A) as well as for the reaction **V** (reoxidation of Q_A^- via an unidentified compound X) and reaction **VII** (reoxidation of PQH_2 via PS I), but all other constants were given values identical with the values used during light exposure. Also, initial concentrations of the reactants were assumed to be equal to the final values obtained after the first light exposure (first hit). The simulation results for the dark period show that after a relatively rapid decrease of the fluorescence (with a duration of 0.1 s) the amplitude remains constant (about 40%). In order to stimulate the decrease of the amplitude of the fluorescence toward zero (i.e., to get all Q_A in the oxidized form), the rate constant for one of the reactions **V** and **VII** (or both of them) should have a non zero value. In Figure 6A the results obtained for the fluorescence dark decay (10 s) with different values of the rate constant of the reaction **V** (0, 5, 10, 15 and 20) are presented. It is obvious from the Figure 6A that the fluorescence dark decay is not linear.

In order to simulate the "second hit" (the fluorescence transient in a second light exposure after a determined dark period), we have used as initial concentrations for the reactants the final concentrations given in our simulation for the dark step, considering the reaction rates to be similar to those of the first light exposure. The curves obtained with our simulation considering different values of the rate constant for reaction **V** are shown in Figure 6B. At values higher than 20 for the rate constant of reaction **V**, the second hit curve matches the first hit curve (apart from a greater value of F_0 for the second hit curve) (see the curve 1). At values less than 20, J and I steps (J more than I) are found to be higher, J being intense so that the I step is less distinctive (see the curves 2-5). The necessary times required to reach these steps are slightly shifted towards higher values. For a zero value of the rate constant corresponding to the reaction **V** in darkness, the simulated curve of the second hit (curve 5) looks like the experimental curve for DCMU, besides the following discrepancies: the initial fluorescence level is higher than F_0, and after the fluorescence reaches the maximum saturation level, a very small decrease towards P level is observed (not easily seen in the curve presented). This

decrease shows us that in normal plants (not inhibited by DCMU), Q_A is not totally reduced at the P level. The initial fluorescence for all these curves (F_0) is higher as the leak of the electrons through the reaction V in darkness is smaller. The P level remains at the same value as in the first hit. These results obtained in our simulations fit quite well the experimental data (see Fig. 7 in /8/). However, often in experimental curves, after reaching the J or I level, there is a decrease of the fluorescence intensity observed (a dip), and so the I step is very well pronounced (see Fig. 1). We have been unable to model this dip until now.

Simulation of the double hit experiment with our complex model yielded results similar to that from individual model (curve 6 in Fig. 7, obtained for a second illumination after 10 sec of darkness with the rate constant k = 5 for reaction V). The redox forms of the $Q_A Q_B$ complex with reduced Q_A have also been simulated (curves 1-5), and it can be seen that there are big differences between their time variation in comparison with the first hit (see Fig. 4B curves 1-5).

CONCLUSIONS

From results presented in this paper, we conclude that the numerical data obtained by the theoretical simulation of the rapid phase of the fluorescence induction with two models — individual and complex — converge already quite well towards the experimental data. The transient phases O, J, I and P have been successfully simulated here. We have also verified the usefulness of the theoretical model by numerical simulation of the experimental results obtained under different environmental conditions.

The results presented show that the numerical simulation by using highly developed software programs is a powerful tool to investigate the dynamics of the primary reactions of photochemistry. We plan to extend our model mainly in two ways: 1) by incorporating reactions on the water-splitting side of photosystem II, and 2) by introducing heterogeneity for different antenna architecture and heterogeneity on the acceptor side of PS II. In this way it should be possible to simulate the fluorescence dynamics of the photosynthetic apparatus under continuous light. Once one arrives at this point the method would become useful to fit all the experimental data, and to evaluate quantitatively the parameters of the model.

ACKNOWLEDGMENT

RÉSUMÉ

La fluorescence variable de la phase rapide de l'induction de la fluorescence de la chlorophylle a est directement liée au transport d'électrons du photosystème II (PS II) des plantes, des algues et des cyanophycées. Nous présentons ici, deux modèles théoriques qui simulent avec succès les valeurs expérimentales de la cinétique d'induction O-J-I-P de la fluorescence en utilisant des réactions du PS II. Les points centraux des deux modèles proposés sont la stabilisation des charges et le processus de double réduction du côté accepteur du PS II. Les suppositions suivantes ont été faites: (1) Les PS II sont homogènes; (2) Les PS II ne sont pas connectés entre eux; et (3) les réactions rédox du PS II suivent une cinétique de premier ordre. Les deux modèles testés sont: (1) le modèle individuel dans lequel les accepteurs d'électrons Q_A et Q_B sont considérés comme étant des unités qui fonctionnent de manière individuelle; (2) le modèle complexe dans lequel les accepteurs d'électrons Q_A et Q_B sont considérés comme étant des unités qui fonctionnent de manière indépendante, dans les centres de réactions.

Les valeurs pour l'analyse dynamique des deux modèles ont été obtenues par intégration numérique des équations différentielles ordinaires (EDO). La procédure *"Livermore Solver of Ordinary Differential Equations with Method Switching"* (LSODA), était incluse dans un logiciel spécialisé de simulation *Gepasi*. Nous avons considéré comme paramètres à introduire les concentrations initiales des réactifs et les constantes de vitesse des réactions rédox.

Nous avons également vérifié nos modèles théoriques en simulant les cinétiques d'induction de la fluorescence dans trois conditions expérimentales différentes: (1) variation de l'intensité lumineuse; (2) traitement du DCMU; et (3) réexposition des échantillons à la lumière actinique après une période définie à l'obscurité (expériences avec illumination double). Les courbes théoriques obtenues s'apparentent bien avec les courbes expérimentales. Ceci prouve que les réactions rédox utilisées dans nos modèles sont adéquates pour décrire le phénomène de l'induction de la fluorescence et que la simulation numérique utilisant des programmes hautement développés est un instrument performant pour investiguer les dynamiques des réactions primaires de la photosynthèse.

REFERENCES

1. PAPAGEORGIOU, G. (1975), "Chlorophyll fluorescence: an intrinsic probe of photosynthesis", in: *Bioenergetics of Photosynthesis* (Edited by Govindjee), Academic Press, New York, pp. 319–371.
2. LAVOREL, J. & A.-L. ETIENNE (1977), "In vivo Chlorophyll Fluorescence", in: *Primary Processes of Photosynthesis* (Edited by J. Barber), Elsevier, North-Holland Biomedical Press, Chapter 6, pp. 203–268.

3. KRAUSE, G.H. & E. WEIS (1991), "Chlorophyll fluorescence and photosynthesis: The basics", *Ann. Rev. Plant. Physiol. Plant. Mol. Biol.*, **42**, 313–349.

4. DAU, H. (1994), "Molecular mechanisms and quantitative models of variable photosystem II fluorescence", *Photochem. Photobiol.*, **60**, 1–23.

5. KAUTSKY, H. & A. HIRSCH (1931), "Neue Versuche zur Kohlensauereassimilation", *Naturwissenschaften*, **48**, 964.

6. STRASSER, R.J. & GOVINDJEE (1991), "The F_0 and the O-J-I-P fluorescence rise in higher plants and algae", in: *Regulation of Chloroplast Biogenesis* (Edited by J.H. Argyroudi-Akoyunoglou), Plenum Press, N.Y., pp. 423–426.

7. STRASSER, R.J. & GOVINDJEE (1992), "On the O-J-I-P fluorescent transient in leaves and D1 mutants of *Chlamydomonas reinhardtii*", in: *Research in Photosynthesis*, Vol. II (Edited by N. Murata), Kluwer Academic Publisher, The Netherlands, pp. 20–32.

8. STRASSER, R.J., A. SRIVASTAVA & GOVINDJEE (1995), "Polyphasic chlorophyll a fluorescence transient in plants and cyanobacteria", *Photochem. Photobiol.*, **61**, 32–42.

9. LATIMER, P., T.T. BANNISTER & E. RABINOWITCH (1956), "Quantum yields of fluorescence of plant pigments", *Science*, **124**, 585–586.

10. HOLZWARTH, A.R. (1991), "Excited-state kinetics in chlorophyll systems and its relationship to the functional organization of the photosystems", in: *Chlorophylls* (Edited by H. Scheer), CRC Press, Inc., London, Section 5, pp. 1125–1152.

11. STRASSER, R.J. (1981), "The Grouping Model of Plant Photosynthesis: Heterogeneity of Photosynthetic units in Thylakoids", in: *Structure and Molecular Organization of the Photosynthetic Apparatus* (Edited by G. Akoyunoglou), Balaban International Science Service, Philadelphia, PA, 727–737.

12. Trissl, H.-W., Y. Gao and K. Wulf (1993), "Theoretical fluorescence induction curves derived from coupled differential equations describing the primary photochemistry of photosystem II by an exciton-radical pair equilibrium", *Biophys. J.*, **64**, 974–988.

13. HSU, B.-D., Y.-S. LEE & O.-R. JANG (1989), "A method for analysis of fluorescence induction curve from DCMU-poisoned chloroplasts", *Biochim. Biophys. Acta*, **975**, 44–49.

14. RENGER, G. & A. SCHULZE (1985), "Quantitative analysis of fluorescence induction curves in isolated spinach chloroplasts", *Photobiochem. Photobiophys.*, **9**, 79–87.

15. HSU, B.-D. (1992), "A theoretical study on the fluorescence induction curve of spinach thylakoids in the absence of DCMU", *Biochim. Biophys. Acta*, **1140**, 30–36.

16. BAAKE, E. & R.J. STRASSER (1990), "A Differential Equation Model for the Description of the Fast Fluorescence Rise (O-I-D-P-Transient) in Leaves", in: *Current research in Photosynthesis* (Edited by M. Baltscheffsky), Kluwer Academic Publishers, Netherlands, Vol. I, 567–570.

17. BAAKE, E. & J.P. SCHLODER (1992), "Modeling the fast fluorescence rise of photosynthesis", *Bull. Math. Biol.*, **54**, 999–1021.

18. GOVINDJEE, J. AMESZ & D.C. FORK (Editors) (1986), *Light Emission by Plant and Bacteria*, Academic Press, Orlando.

19. STRASSER, R.J. & H. GREPPIN (1981), "Primary Reactions of Photochemistry in Higher Plants", in: *Structure and Molecular Organization of the Photosynthetic Apparatus* (Edited by G. Akoyunoglou), Balaban International Science Service, Philadelphia, PA, 717–726.

20. STIEHL, H.H. & H.T. WITT (1969), "Quantitative treatment of the function of plastoquinone in photosynthesis", *Z. Naturforsch. Teil B*, **24**, 1588–1598.

21. HAEHNEL, W. (1984), "Photosynthetic electron transport in higher plants", *Ann. Rev. Plant. Physiol.*, **35**, 659–693.

22. MALKIN, S. & B. KOK (1966), "Fluorescence induction studies in isolated chloroplasts. I, Number of components involved in the reaction and quantum yields", *Biochim. Biophys. Acta*, **126**, 413–432.

23. DUYSENS, L.M.N. & H.E. SWEERS (1963), "Mechanism of the two photochemical reactions in algae as studied by means of fluorescence", in: *Studies on Microalgae and Photosynthetic Bacteria* (Ed. Japanese Society of Plant Physiologists), University of Tokyo Press, Tokyo, pp. 353–372.

24. BUTLER, W.L. (1972), "On the primary nature of fluorescence yields changes associated with photosynthesis", *Proc. Natl. Acad. Sci. USA*, **69**, 3420–3422.

25. DEPREZ, J., A. DOBEK, N.E. GEACINTOV, G. PAILLOTIN & J. BRETON (1983), "Probing fluorescence induction in chloroplasts on a nasosecond time scale utilizing picosecond laser pulse pairs", *Biochim. Biophys. Acta*, **752**, 444–454.

26. SONNEVELD, A., H. RADEMAKER & L.N.M. DUYSENS (1979), "Chlorophyll a fluorescence as a monitor of nanosecond reduction of the photooxidized primary donor P-680$^+$ of photosystem II", *Biochim. Biophys. Acta*, **548**, 536–551.

27. HOGANSON, C.W., P.A. CASEY & O. HANSSON (1991), "Flash photolysis studies of manganese-depleted photosystem II: evidence for binding of MN^{2+} and other transition metal ions", *Biochim. Biophys. Acta*, **1057**, 399–406.

28. DEBUS, R.J. (1992), "The manganese and the calcium ions of photosynthetic oxygen evolution", Biochim. *Biophys. Acta*, **1102**, 269–352.

29. Gepasi is a software package for the simulation of metabolic models, both of their transient (dynamic) or steady state. Author: Pedro Mendes, University of Wales, Department of Biological Sciences, Aberystwyth, Dyfed, SY23 3DA, United Kingdom. It is a free software package available from several archives in the Internet or other networks.

30. GNUPLOT is a command-driven interactive function plotting program and represents the work of many people. It is a free software package available from several archives in the Internet or other networks.

31. PETZOLD, L. (1983), "Automatic selection of methods for solving stiff and nonstiff systems of ordinary differential equations", *SIAM. J. Sci. Stat. Comput.*, **4**, 136–448.

32. GEAR, C.W. (1971), in: *Numerical initial value problem of ordinary differential equations*, Prentice-Englwood Cliffs, N.J.

33. HINDMARSCH, A.C. (1980), "LSODE and LSOI, two initial value of ordinary differential equation solvers", *A.C.M. Signum Newsletter*, **15**, 4 December, 10–11.

34. JOLIOT, P. & A. JOLIOT (1992), "Electron transfer between Photosystem II and the cytochrome b/f complex: mechanistic and structural implications", *Biochim. Biophys. Acta*, **1102**, 53–61.

35. ROBINSON, H.H. & A.R. CROFTS (1984), "Kinetics of proton uptake and the oxidation-reduction reactions of the quinone acceptor complex of PS II from pea chloroplasts", in: *Advances in Photosynthesis Research* (Edited by C. Sybesma), Martinus Nijhoff/Dr. W. Junk, The Hague, Vol. 1, pp. 477–480.

36. GOBINDJEE & M.R. WASIELEWSKI (1989), "Photosystem II: from a femtosecond to a millisecond", in: *Plant Biology Photosynthesis* (Edited by W.R. Briggd), Alan R. Liss, Inc., Vol. 8, pp. 71–103.

37. RICH, P.R. & D.A. MOSS (1987), "The Reactions pf Quinones in Higher Plant Photosynthesis", in: *The Light Reactions* (Edited by J. Barber), Elsevier Science Publishers B.V. (Biochemical Division), Chapter 10, pp. 421–445.

38. CROFTS, A.R. & C.A. WRAIGHT (1983), "The electrochemical domain of photosynthesis", *Biochim. Biophys. Acta*, **726**, 149–185.

39. CRAMER, W.A. & D.B. KNAFF (1990), "The quinone connection", in: *Energy Transduction in Biological Membranes* (Edited by C.R. Cantor), Springer-Verlag, New York, Berlin, Heidelberg, Chapter 5, pp. 193–238.

40. CROFTS, A.R., H.H. ROBINSON & M. SNOZZI (1984), "Reactions of quinones at catalytic sites: a diffusional role in H-transfer", in: *Advances in Photosynthesis Research* (Edited by C. Sybesma), Nijhoff/W. Junk, The Hague, I, pp. 461–468.

41. VELTHUYS, B.R. (1981), "Electron transport dependent competition between plastoquinone and inhibitors for binding to photosystem II", *FEBS Lett.*, **126**, 277–281.